General and Comparative Endocrinology 160 (2009) 194–204

Contents lists available at ScienceDirect

General and Comparative Endocrinology

journal homepage: www.elsevier.com/locate/ygcen

Sex and temporal variations of the vasotocin neuronal system in the damselfish brain

Karen P. Maruska *

Department of Zoology, University of Hawai'i at Manoa, 2538 The Mall, Honolulu, HI 96822, USA
Hawai'i Institute of Marine Biology, 46-007 Lilipuna Rd., Kaneohe, HI 96744, USA

ARTICLE INFO

Article history:
Received 30 July 2008
Revised 26 October 2008
Accepted 18 November 2008
Available online 3 December 2008

Keywords:
Acoustic
AVT
Immunocytochemistry
Midbrain
Seasonal
Neuromodulation
Sensory
Torus Semicircularis
Vagal

ABSTRACT

The neuropeptide vasotocin (VT) is an important regulator of reproduction and social behaviors, and hypothesized to function as a neuromodulator of sensory and motor processing. In adult fishes, VT is primarily produced in three different cell groups (parvocellular, magnocellular, and gigantocellular) within preoptic nuclei, but little is known about sex and seasonal variations of these somata and their relationship to sensory and motor processing. I used immunocytochemistry to (1) test for sex and seasonal variations in VT-immunoreactive (-ir) somata number, size, and fiber densities in the brain of a soniferous damselfish, and (2) test the hypothesis that VT-ir axons project to and vary seasonally in sensory and motor regions of the brain. Sex differences in somata number and size were restricted to parvocellular neurons, while seasonal variations were found within parvocellular and gigantocellular, but not magnocellular neurons. Both males and females had more gigantocellular neurons during peak spawning compared to other times. VT-ir fibers were most abundant in sensory and motor processing regions of the auditory-mechanosensory torus semicircularis (TS), facial lobe, and vagal motor nucleus (VMN), while sparse innervation was found to the tectum and hindbrain auditory and mechanosensory nuclei. VT-ir fiber densities in the TS and VMN were higher during peak spawning, and correlated with gigantocellular (TS, VMN) and parvocellular (TS) somata number. These results provide neuroanatomical support for a relationship between temporal changes in specific VT somata and projections to some sensory and motor processing regions in the damselfish brain that may influence complex communicative and social behaviors.

1. Introduction

The neuropeptide vasotocin (VT) and its mammalian homolog vasopressin (VP) are broadly distributed throughout the vertebrate brain and important regulators of complex sex-typical, species-specific, and context-specific social and reproductive behaviors such as aggression, parental care, courtship, and social recognition (see Goodson and Bass, 2001; Lim and Young, 2006 for reviews). In addition to projections to the pituitary and forebrain, VT and VP neurons also have prominent projections to midbrain and hindbrain regions where the peptide is hypothesized to function as a neuromodulator or modulatory neurotransmitter. While the distribution and behavioral functions of VT and VP are relatively well-studied with regard to endocrine and reproductive activities (see Goodson and Bass, 2001), less is known about their role(s) in modulation of sensory, motor, or sensorimotor function (Rose and Moore, 2002).

Several previous studies have provided support for VT and VPs neuromodulatory function in vertebrates. For example, VT and VP were shown to influence sensorimotor processing, and visual, olfactory, somatosensory, and vocal-acoustic reproductive behaviors (e.g. Goodson and Bass, 2001; Rose and Moore, 2002). Further, Rose and Moore (2002; Moore and Rose, 2002) proposed the *sensorimotor processing hypothesis* based on their roughskin newt (*Taricha granulosa*) model, which states that VT and VP act centrally to influence regions of sensory and motor processing to modulate behaviors, and Thompson et al. (2008) recently showed that VT affects how sensory information is translated into motor output. In order for VT or VP to modulate behaviors via sensory or motor circuitry, the regions of the brain that process behaviorally-relevant sensory input and motor output should contain VT or VP axons, terminal fields, and target cells that express VT or VP receptors. However, few studies have quantitatively tested these predictions and examined the distribution of VT or VP or their receptors with special emphasis on sensory and motor regions of the brain.

Fishes have specific social and reproductive behaviors associated with distinct annual cycles that are known to be influenced

* Address: Biology Department, Stanford University, 371 Serra Mall, Gilbert Bldg., Stanford, CA 94305, USA.
E-mail address: maruska@stanford.edu

0016-6480/$ - see front matter © 2008 Elsevier Inc. All rights reserved.
doi:10.1016/j.ygcen.2008.11.018

by VT. Previous studies on VT in fishes concentrate on neuronal sexual dimorphisms in sex-changing species (e.g. wrasses, gobies) and those with alternative reproductive morphs (e.g. midshipman, blennies, African cichlid) (Foran and Bass, 1998; Godwin et al., 2000; Grober et al., 2002; Miranda et al., 2003; Greenwood et al., 2008). An association between the expression of alternative tactics and forebrain VT is found in all species examined to date (see Foran and Bass, 1999; Oliveira et al., 2005), but less is known about sex and temporal variations in the VT system of adult gonochoristic fishes that do not have alternative reproductive morphs (Parhar et al., 2001). In addition, little is known about the differential projections, sex and seasonal changes, and function of the three different VT cell groups found in fishes (parvocellular, magnocellular, and gigantocellular). Fishes use a combination of visual, auditory, olfactory, and mechanosensory cues to coordinate intra and interspecific social behaviors, and VT has the potential to influence this sensory and motor processing on a temporal basis. Thus monitoring changes in fiber densities and somata in the three separate cell groups over reproductive and non-reproductive seasons can also specify the period of the reproductive cycle that VT may influence sensory, motor, and behavioral circuits.

Coral reef fishes provide excellent comparative models for the action of neuropeptides on behaviors and sensory and motor modulation because they represent a large diverse group of vertebrates, show varied social behaviors among closely related species, have separate and distinct neuropeptide populations, and use multiple sensory cues for social interactions. The Hawaiian sergeant damselfish *Abudefduf abdominalis* is a member of the soniferous family Pomacentridae (~321 species in 28 genera) that displays temporally and sexually diverse social behaviors. This species is colonial and aggregates in the water column in mixed sex schools with limited aggressive interactions during non-reproductive times. During the spawning season, males clean and prepare a benthic substrate and engage in nest defense and courtship displays that include coloration changes and sound production to attract a female to the nest for spawning (Helfrich, 1958; Maruska et al., 2007a). In addition to visual cues, agonistic and reproductive interactions in this species involve important sensory signals detected by both the lateral line and inner ear (sound production and hydrodynamic flow generated by body and fin movements). Thus, the temporally and sexually diverse social behaviors of this species provide an ideal model to test for both peptide-sensory convergence in behaviorally-relevant brain centers, and correlations with sex and seasonal changes in behavior.

The goals of this study were several-fold. First, I examine the VT neuronal system with immunocytochemistry to test for sexual dimorphism and temporal changes in neuropeptide somata within the brain of a gonochoristic teleost that does not express alternative reproductive morphs. Second, I test the prediction that VT-containing axons project to specific behaviorally-relevant sensory and motor processing regions of the fish brain. I concentrate on octavolateralis (auditory and lateral line) processing regions because of VT's known role in vocal-acoustic behaviors (Goodson and Bass, 2001) and the importance of acoustic and hydrodynamic communication in the study species (Maruska et al., 2007a). Third, the density of VT-ir axons within specific sensory and motor regions was compared among sexes and reproductive seasons to test for sex-specific temporal variations in VT's ability to potentially modulate behavior via sensory or motor circuits. Sex and seasonal quantification of VT-ir fiber projections to caudal brain regions have not previously been examined in teleost fishes. Results of this study demonstrate both sex and seasonal variations in VT-ir somata, and fiber densities in behaviorally-relevant sensory and motor regions of the damselfish brain. Future physiological and behavioral studies are needed to test the neuromodulatory functions of VT on sensory processing and natural behaviors.

2. Materials and methods

2.1. Animals and tissue preparation

Adult Hawaiian sergeant fish *Abudefduf abdominalis* were collected via hook and line from Kane'ohe Bay, Oahu, transported to the laboratory and perfused immediately (average time between capture and anesthesia was 15 min). Hawaiian sergeant fish show some spawning activity year-round, but there is an increase in reproductive activities and gonadosomatic index (GSI) in spring and summer followed by reduced activity and GSI in fall and winter (Helfrich, 1958; Maruska, 2007). As a result, sexually mature adult males and females (standard length $\geqslant$ 110 mm) were collected from four separate time periods in order to reduce the chances of missing seasonal variations by examination of only peak and minimal spawning times (see Maruska et al., 2007b). Fish were collected in January (pre spawn), April (early spawn; rising gonadal indicies), June (peak spawn; maximum gonadal indicies), and October (post spawn; minimal gonadal indicies) based on previous reproductive analyses of this population (Helfrich, 1958), examination of gonad size and gamete maturation, and qualitative observations of reproductive behaviors in the wild (Maruska, 2007). Fish were anesthetized with MS-222, measured for standard length (SL) and total length (TL) to the nearest 0.5 mm, and body weight (BW) to the nearest 0.1 g. Sex was determined by examination of their sexually dimorphic urogenital papilla, and verified by examination of gonadal tissue under a compound microscope at 400×. Fish were perfused transcardially with 0.9% heparinized saline followed by 4% paraformaldehyde in 0.1 M phosphate buffer (PB). Brains were removed, postfixed in 4% paraformaldehyde in 0.1 M PB at 4 °C for 24 h, rinsed in 0.1 M PB, and cryoprotected overnight in 30% sucrose in 0.1 M PB prior to sectioning. Collection, maintenance, surgical, and perfusion procedures for fish used in this study were approved by the University of Hawai'i Institutional Animal Care and Use Committee.

2.2. Immunocytochemistry

Cryoprotected brains were embedded in Histoprep mounting media (Fisher Scientific) and sectioned in the sagittal or transverse plane at 24 μm with a cryostat. Alternate sections were collected onto chrom-alum-coated slides, dried flat overnight at room temperature, and stored at 4 °C prior to immunocytochemical processing. Mounted brain sections were brought to room temperature (20–22 °C), surrounded with a hydrophobic barrier (Immedge pen; Vector Laboratories), rinsed with 0.05 M phosphate buffered saline (PBS; pH 7.4) (2 × 15 min), blocked for 1 h with 2% normal goat serum (NGS; Vector Laboratories) in PBS containing 0.3% Triton-X 100 (Sigma), and incubated with primary antibody (rabbit anti-VT, 1:5000 final concentration, donated by Dr. Matthew Grober, Georgia State University, USA) overnight (14–16 h) at room temperature in a sealed humidified chamber. Primary antibody incubation was followed by a PBS wash (2 × 15 min), incubation with biotinylated goat anti-rabbit secondary antibody (Vector Laboratories) in PBS with 2% NGS for 1 h, PBS wash (2 × 15 min), quenching with 1.5% hydrogen peroxide in PBS for 15 min, PBS wash (2 × 15 min), incubation with avidin-biotin-horseradish peroxidase complex (ABC Elite kit; Vector Laboratories) for 2 h, PBS wash (2 × 15 min), and reacted with a diaminobenzidine (DAB) chromogen substrate kit with nickel chloride intensification (Vector Laboratories) for 5 min. Slides were then soaked in distilled water for 10 min to stop the reaction, lightly counterstained with 0.1% methyl green, dehydrated in an ethanol series (50–100%), cleared in toluene, and coverslipped with Cytoseal 60 mounting media (Richard Allen Scientific).

Immunocytochemistry controls included: (1) omission of primary antisera, secondary antisera, ABC solution or DAB all resulted in no staining, (2) preabsorption of anti-VT with 8 μM VT peptide (Sigma) eliminated all reaction product, and (3) the potential cross-reactivity of the VT antibody with isotocin was tested by incubation of alternate sections with plain anti-VT and anti-VT preabsorbed with 8 μM isotocin peptide (Bachem). This control showed that there was no difference in the number of labeled somata and fibers between alternate sections reacted with plain anti-VT and anti-VT preabsorbed with isotocin (Student's *t*-tests, $p > 0.05$), thus demonstrating no cross-reactivity of the VT antibody with isotocin-containing neurons. Brain sections were observed on a Zeiss Axioskop 2 microscope and images captured with an Optronics Macrofire digital camera. Line illustrations were made with a drawing tube on an Olympus BH2 microscope.

2.3. Quantification of VT somata

Unbiased estimates of the number and size of VT cells were acquired by quantification of sagittal sections without knowledge of SL, BW, sex, or month collected. Nomenclature of the diencephalon follows that of Braford and Northcutt (1983). Each VT-ir soma was assigned to either the parvocellular (included nucleus preopticus parvocellularis anterioris [PPa][1] and posterioris [PPp], and nucleus preopticus magnocellularis pars parvocellularis [PMp]), magnocellular (nucleus preopticus magnocellularis pars magnocellularis [PMm]), or gigantocellular (nucleus preopticus magnocellularis pars gigantocellularis [PMg]) cell group based on neuroanatomical location, somata morphology, and size (Braford and Northcutt, 1983). An additional VT-ir cell group was present in the ventral tuberal hypothalamus of the Hawaiian sergeant, as mentioned in other fish studies (Goodson and Bass, 2000; Greenwood et al., 2008; Dewan et al., 2008), but was not quantified due to inconsistent label and presence in only some individuals. To assess whether somata could be counted more than once in adjacent alternate sagittal sections, ten randomly chosen cell diameters from each cell group in three fish were measured along the medial-lateral brain axis in transverse sections. The largest cells were the gigantocellular VT neurons, which were approximately equal to section thickness ($\bar{x}$ diam. = 25.3 ± 0.6 μm SE). Thus, there was no duplication of cell counts made on alternate 24 μm sections.

Cell size was determined from digital images of somata at 400× and cell profile area was calculated with Sigma Scan Pro 5.0 (SPSS, Inc.). For each fish, 10 randomly chosen VT cells were measured within the same preoptic nuclei among individual fish. Cell profile areas were measured at a point where the labeled cell perimeter was easily discernable and a distinct nucleus with at least one neurite was visible, with the exception of parvocellular neurons where cell nuclei were often not visible and only the criteria of a discernable perimeter and neurite presence were used. Mean VT cell profile area (μm^2) in the sergeant fish differed among parvo, magno, and gigantocellular somata (1-way analysis of variance [ANOVA], $p < 0.001$; Tukey's test $p < 0.05$) in the following order: parvo < magno < giganto, which served as a further character to distinguish these cell groups.

2.4. Quantification of VT-immunoreactive axons within motor and sensory regions

The density of VT-ir fibers was quantified in sagittal sections to test for sex and seasonal variations in innervation to sensory and motor regions. Gray-level thresholding with Scion Image software (NIH) was performed in both the caudal-lateral torus semicircularis (TS; midbrain auditory and lateral line processing region) and vagal motor nucleus (VMN; efferent neurons that innervate striated muscles of the pharynx and gills, as well as coelomic organs including the swim bladder, heart, and gastrointestinal tract) of each animal from photomicrographs taken at 400× of a 360 μm^2 area in each region. Measurements were performed at the same location in each region among individuals based on neuroanatomical landmarks without knowledge of fish sex, size, or season. Photographs were all taken at the same time with identical camera and software settings. The number of pixels covered by immunoreactive fibers was then determined from a single section in each animal and expressed as a percentage of the 360 μm^2 area covered by VT-ir fibers. VT-ir fibers within the primary hindbrain mechanosensory and octaval nuclei were scattered and difficult to quantify, so are only qualitatively described in Section 3.

2.5. Statistical analyses

Linear regressions for all subjects pooled together were initially used to test for effects of fish body size on cell number and cell size within each VT-ir cell group because the data did not meet the assumption of parallel slopes required for analysis of covariance. This regression analysis revealed only a single positive relationship between body size and gigantocellular somata size (linear regression, $r^2 = 0.22$, $p = 0.001$). However, when separated by sex and season, there were no significant relationships between body size and cell number or cell size in any of the three VT-ir cell groups, including the gigantocellular (linear regressions, $p > 0.05$). To verify that the seasonal variations in gigantocellular neuron number were not influenced by body size differences, the effects of body size were factored out with the following equation (as described in Greenwood et al., 2008): $SSc = SSu + \{[(SSu \times SLx/SL) - SSu] \times K\}$, where SSc, corrected mean soma size for an individual fish; SSu, uncorrected mean soma size for an individual fish; SL, the individual fish standard length; SLx, mean standard length for the subject pool under investigation; and *K*, Pearson's *r* determined from a Pearson Product Moment correlation test for that sample. This analysis showed that the seasonal differences in gigantocellular neurons were identical whether the data were corrected or uncorrected. Therefore, because the goal of this study was to examine variations in VT-ir somata number and size between sexes and among seasons, and there was no relationship between body size and cell characters when separated by sex and season, the data are presented and interpreted without any adjustment for body size. Differences in the number and size of VT-ir somata and fiber densities were determined with a two-way ANOVA with sex and season as factors, and subsequent Tukey's tests for all pairwise comparisons. In some cases, data were normalized by a log transformation prior to testing. Pearson Product Moment Correlation was used to test for correlations between VT-ir fiber densities and somata number and size within each VT cell group. All statistical analyses were performed with SigmaStat 3.1 (Systat, Inc.).

[1] *Abbreviations used:* 4v, 4th ventricle; AP, area postrema; CC, cerebellar crest; CCe, corpus cerebelli; CE, cerebellum; Dc, central zone of area dorsalis telencephali; Dl, lateral zone of area dorsalis telencephali; Dm, medial zone of area dorsalis telencephali; Dp, posterior zone of area dorsalis telencephali; EG, eminentia granularis; FL, facial lobe; G, nucleus glomerulosus; Ha, habenula; HYP, hypothalamus; IL, inferior lobe of hypothalamus; M, medulla; MON, medial octavolateralis nucleus; NRLl, nucleus recessus lateralis, pars lateralis; nX, cranial nerve X, vagus nerve; OB, olfactory bulb; ON, optic nerve; PC, posterior commissure; PHT, preoptico-hypophyseal tract; PLLn, posterior lateral line nerve; PMg, nucleus preopticus magnocellularis pars gigantocellularis; PMm, nucleus preopticus magnocellularis pars magnocellularis; PPa, nucleus preopticus parvocellularis anterioris; PPp, nucleus preopticus parvocellularis posterioris; RF, reticular formation; sgt, secondary gustatory tract; SV, saccus vasculosus; T, tectum; Teg, tegmentum; TEL, telencephalon; TL, torus longitudinalis; TLa, nucleus tori lateralis; TS, torus semicircularis; TTB, tractus tectobulbaris; VCe, valvula cerebelli; Vd, dorsal zone of area ventralis telencephali; VL, vagal lobe; VMN, vagal motor nucleus; Vv, ventral zone of area ventralis telencephali.

3. Results

3.1. Distribution

VT-ir somata are found within preoptic nuclei of the damselfish brain (Figs. 1A and B). The majority of parvocellular neurons were found within the PPa, but some labeled neurons were also found within the PPp and PMp. Parvocellular neurons were the most rostral and numerous, round or oval in shape, monopolar, of small diameter ($\bar{x}$ diam. = 7.9 ± 0.30 μm SE, n = 10 cells, 3 fish), and extended more laterally than either the magnocellular or gigantocellular VT-ir somata groups (Figs. 1A–C and 2B). The magnocellular neurons were located in the PMm immediately caudal to the PMp, approximately twice the size of parvocellular somata ($\bar{x}$ diam. = 16.4 ± 0.30 μm SE, n = 10 cells, 3 fish), and were multi or monopolar (Figs. 1A–B, D, and 2B–C). The gigantocellular neurons were found most caudal in the PMg along a dorso-ventral band that extended from above the PMm region ventrally into the rostral hypothalamus, and were 2–2.5 times larger than the magnocellular somata ($\bar{x}$ diam. = 25.3 ± 0.60 μm SE, n = 10 cells, 3 fish) (Figs. 1A–B, E–G, and 2D). These cells were multipolar with multidirectional processes that appeared to project both towards the pituitary and caudal brain regions (Figs. 1E–G). Gigantocellular somata also had large diameter processes that often contained many spines along their length (Fig. 1G).

The highest density of VT-ir axons formed a dense preoptico-hypophyseal tract (PHT) that coursed ventro-lateral from the preoptic area along the rostral hypothalamus to the pituitary (Figs. 1A, 2D, and 3C). Sparse fibers were observed in the olfactory bulbs, area dorsalis telencephali, thalamic nuclei and hypothalamus (Figs. 1A and 2A–D). The most abundant VT projections in the forebrain were to the area ventralis telencephali and preoptic nuclei (Figs. 2A–D). In the midbrain, VT-ir axons were most abundant in the tegmentum and torus semicircularis (Figs. 2D–F and 3E). Only sparse VT-ir fibers were found in the deep layers of the tectum (e.g. stratum album centrale), but they occurred in the same region of dense gonadotropin-releasing hormone (GnRH)-ir projections in this species (Maruska and Tricas, 2007). Sparse VT-ir fibers occurred in both the valvula and corpus granular layer of the cerebellum. VT-ir fibers projected through the midbrain to the medulla and spinal cord in a lateral rostro-caudal tract (Figs. 2E–J and 3D), and the VT-ir fibers in this hindbrain tract were of smaller diameter and contained numerous varicosities (i.e. swellings) compared to the larger diameter non-varicose fibers of the PHT (compare Figs. 3C and D). VT-ir fibers were also found within the facial lobe, sensory vagal lobe, and secondary gustatory tract (Fig. 2H). In the caudal brain, VT-ir axons were abundant in the ventral medulla and nuclei of the reticular formation, and some scattered fibers found within octavolateralis nuclei (Fig. 2G–I). VT-ir fibers were also abundant within the VMN and varicose fibers appeared to make synaptic contacts with cell bodies in this region (see below; Figs. 2I, and 3A, F). Caudal to the fourth ventricle at the junction of the caudal medulla and rostral spinal cord, the lateral VT-ir tract coursed medial and dorsal to form a dense plexus of beaded fibers along the dorsal midline near the area postrema (Figs. 2J and 3B).

3.2. Sex and seasonal variations in VT-ir somata

A total of 45 fish ($\bar{x}$ SL = 124.2 ± 7.5 mm SD; $\bar{x}$ BW = 83.6 ± 15.9 g SD) were used to test for sex and seasonal variations in VT-ir somata number and size. There was no difference in body size (SL or BW) among sexes or among the four sampling periods (2-way ANOVA, F_{season} = 0.55, p = 0.65; F_{sex} = 0.41, p = 0.53). Thus any sex or seasonal variations in VT-ir cells or fibers are not due to a size sample bias within a sex or sampling period.

Sex differences in VT-ir cell number were restricted to parvocellular neurons (Fig. 4). Males had more parvocellular somata during the post spawn period compared to females (2-way ANOVA, F_{sex} = 14.53, p < 0.001; Tukey's test, p = 0.02) and females had larger parvocellular somata during the pre spawn period compared to males (2-way ANOVA, F_{sex} = 4.61, p = 0.04; Tukey's test, p = 0.03) (Fig. 4).

Seasonal variations were observed for both parvocellular and gigantocellular VT-ir groups, but not magnocellular (Fig. 4). Male fish had more parvocellular somata during the post spawn period compared to pre and early spawn times (2-way ANOVA, F_{season} = 5.73, p = 0.003; Tukey's tests, p = 0.01 pre spawn; p = 0.04 early spawn). In addition, females had smaller parvocellular somata during post spawn compared to pre and early spawn times (2-way ANOVA, F_{season} = 4.60, p = 0.01; Tukey's test, p = 0.04 pre spawn; p = 0.004 early spawn). There were no seasonal variations in the number or size of magnocellular somata for males or females (2-way ANOVA, F_{season} = 1.09, p = 0.37 number; F_{season} = 2.49, p = 0.08 size). In the PMg, both males and females had more gigantocellular somata during the peak spawn period compared to all other times (2-way ANOVA, F_{season} = 11.63, p < 0.001; Tukey's tests, p < 0.05) (Fig. 4). A seasonal variation in the size of gigantocellular somata was also detected (2-way ANOVA, F_{season} = 4.12, p = 0.013), but post-hoc tests did not resolve differences among the four sampling periods (Tukey's tests, p > 0.05) (Fig. 4).

3.3. VT-immunoreactivity in motor and sensory regions

VT-ir axons were found within several motor and octavolateralis sensory regions of the midbrain and hindbrain. In the tectum, VT-ir axons were virtually absent from the dorsal visual layers of the stratum marginale (SM), stratum opticum (SO), and stratum fibrosum et griseum superficiale (SFGS), and sparse in the deeper multimodal layers of the stratum griseum centrale (SGC) and stratum album centrale (SAC). In contrast, VT-ir fibers were more abundant within the TS (auditory and lateral line processing region) (Figs. 2D–F and 3E). In the TS, scattered small diameter VT-ir fibers were found in both the dorsal and ventral regions throughout its rostro-caudal length, but were more abundant in the caudal TS. In the hindbrain, VT-ir fibers were sparse within the medial octavolateralis nucleus (MON; lateral line processing region) and all auditory nuclei (descending, anterior, magnocellular, tangential, and posterior octaval nuclei). In contrast, VT-ir fibers were more abundant in the facial lobe, secondary gustatory tract, and sensory vagal lobe. VT-ir fibers were also abundant within the VMN and glossopharyngeal motor nucleus of the caudal medulla. The lateral rostro-caudal VT tract that projects to the hindbrain turns medial at the level of the VMN and numerous putative terminals (varicosities) surround the large motor neurons (Figs. 3A and F).

3.4. Sex and seasonal variations in VT-ir fiber densities

The density of VT-ir axons also showed sex and seasonal variations within the TS of the midbrain and VMN of the hindbrain (Fig. 5). However, there were no relationships between fiber density (TS or VMN) and body size (BW or SL) for either sex during any time period (linear regressions, p > 0.05). In the TS, females had a higher density of VT-ir fibers during peak spawn compared to males (2-way ANOVA, F_{sex} = 5.6, p < 0.001; Tukey's test, p < 0.001) (Fig. 5A). Females also had a greater density of VT-ir fibers during peak spawn compared to all other times (2-way ANOVA, F_{season} = 13.61; p < 0.001; Tukey's tests, p < 0.001). There were no seasonal differences within the TS for males (Tukey's tests, p > 0.05) (Fig. 5A).

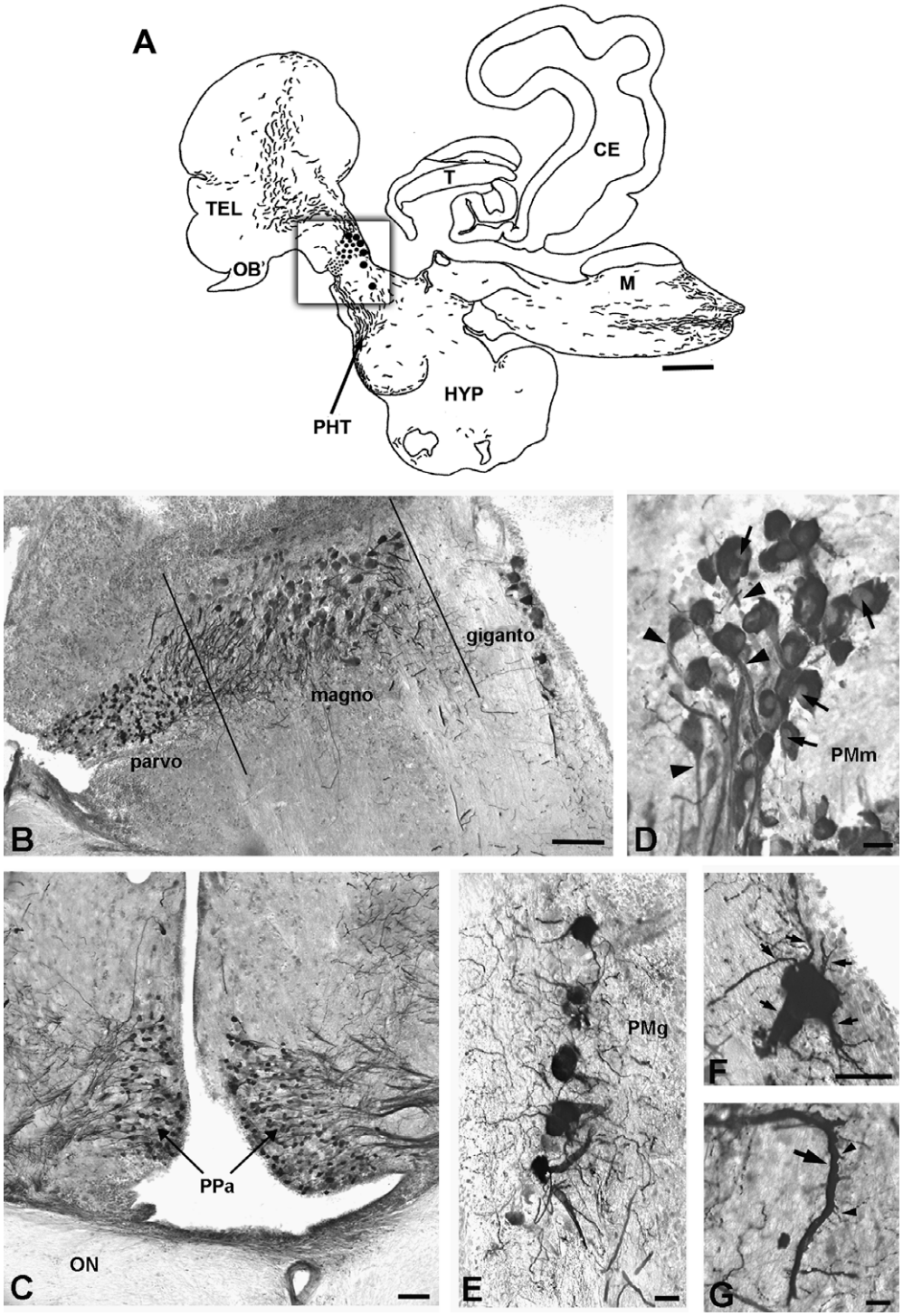

Fig. 1. VT-immunoreactive (-ir) somata and axons in the brain of the Hawaiian sergeant fish, *Abudefduf abdominalis*. (A) Camera lucida drawing of a representative mid-sagittal section through the brain shows the location of VT-ir somata located in parvocellular (small dots), magnocellular (medium dots), and gigantocellular (large dots) groups within the preoptic nuclei (see text for descriptions). (B) Representative photomicrograph of the boxed region in A shows the VT-ir parvo, magno, and gigantocellular somata. Lines delineate the approximate divisions between cell groups in this sagittal section. Rostral is to the left. (C) Transverse section through the nucleus preopticus parvocellularis anterioris (PPa) shows the small, numerous, monopolar parvocellular VT-ir neurons. ON, optic nerve. (D) Magnocellular VT-ir neurons in the nucleus preopticus magnocellularis pars magnocellularis (PMm) are twice as large as parvocellular neurons and often contain a single axon (arrowheads) with a large prominent nucleus visible within the cell body (arrows). (E) Gigantocellular VT-ir neurons are found in a dorso-ventral band within the nucleus preopticus magnocellularis pars gigantocellularis (PMg). (F) Gigantocellular VT-ir neurons are large with multiple processes (arrowheads) that extend in many directions. (G) Gigantocellular neurons also often contain a large diameter process (large arrow) with several small varicose extensions or spines (small arrows). CE, cerebellum; HYP, hypothalamus; M, medulla; OB, olfactory bulb; PHT, preoptico-hypophyseal tract; T, tectum; TEL, telencephalon. Scale bars = 1 mm (A); 100 μm (B); 50 μm (C); 15 μm (D and G); 30 μm (E and F).

The density of VT-ir fibers in the TS was also negatively correlated with the number of parvocellular somata in all fish together, and positively correlated with the number of gigantocellular somata in all fish together (Fig. 6A and B), as well as in females alone (Pearson Product Moment Correlation, $r = 0.50$, $p = 0.02$). In contrast, the density of VT-ir fibers in the TS was not correlated

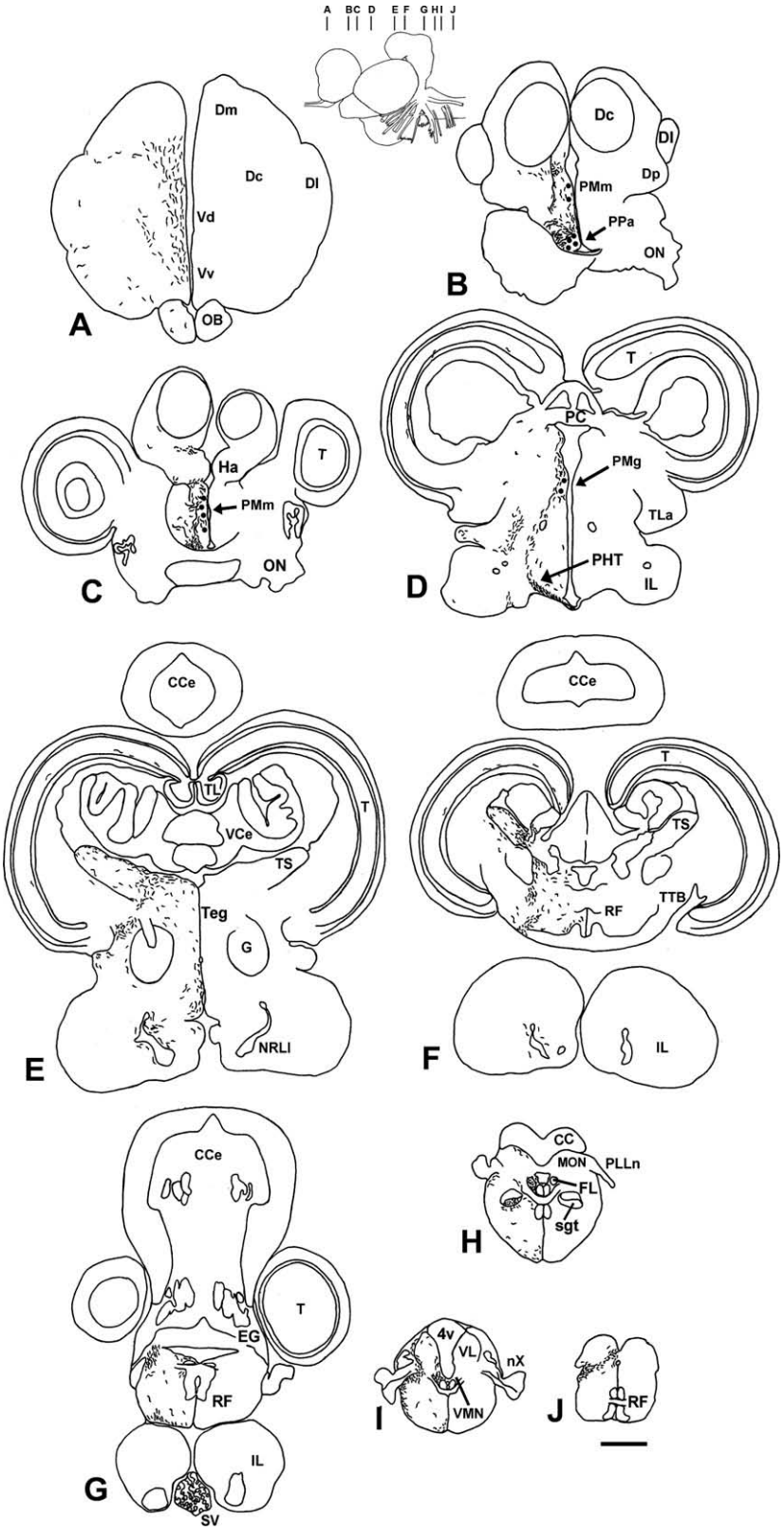

Fig. 2. Distribution of VT-immunoreactive (-ir) neurons in the brain of the Hawaiian sergeant fish, *Abudefduf abdominalis*. Camera lucida drawings of representative transverse sections through the brain show the locations of VT-ir somata (dots) and fibers (lines). VT-ir somata are located in preoptic nuclei, while immunoreactive axons are found primarily in the ventral telencephalon, preoptic area, hypothalamus, midbrain tegmentum, torus semicircularis, torus lateralis, tectum, reticular formation, and sensory and motor regions of the hindbrain. Inset shows the approximate location of each cross section. See list for abbreviations. Scale bar = 1 mm.

with somata number or size in any of the cell groups for males (Pearson Product Moment Correlation, $p > 0.05$).

In the VMN, males had greater VT-ir fiber densities during pre, peak and post spawn periods compared to females (2-way ANOVA,

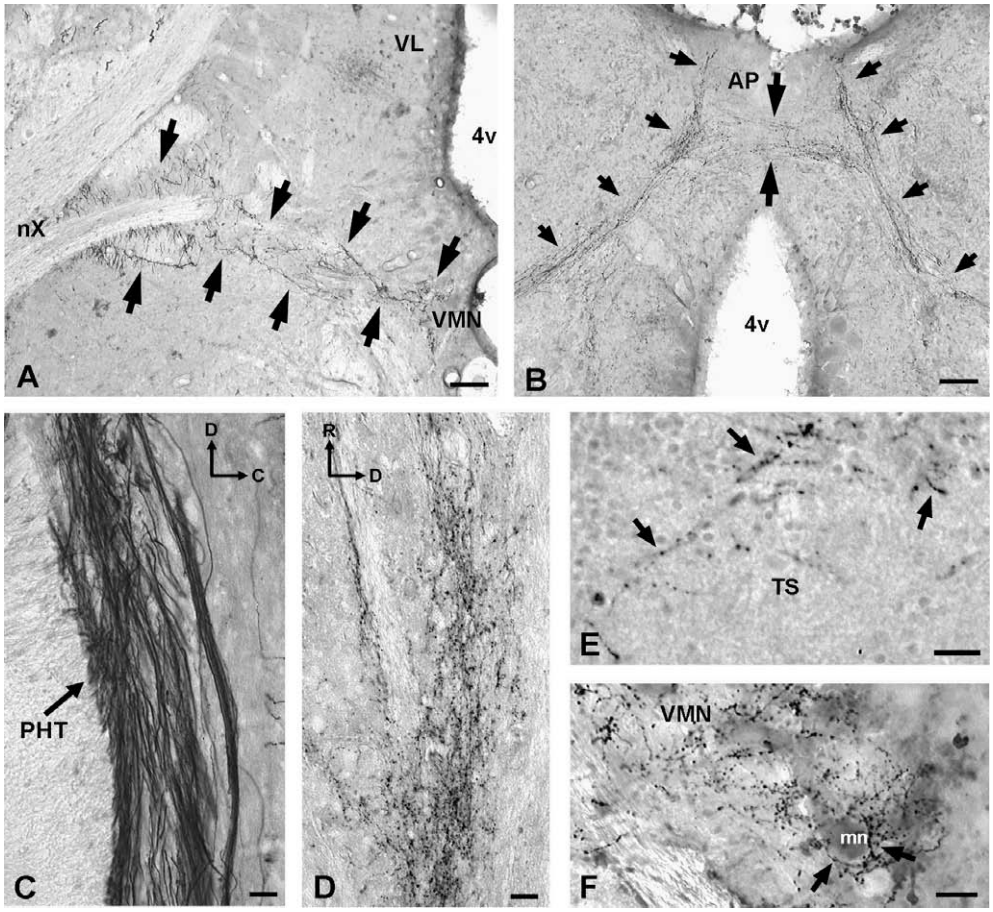

Fig. 3. VT-immunoreactive (-ir) axons in the brain of the Hawaiian sergeant fish, *Abudefduf abdominalis*. (A) Transverse section through the hindbrain shows the lateral VT-ir fiber tract around cranial nerve X (nX) as it courses medially (arrows) to terminate around motor neurons within the vagal motor nucleus (VMN). (B) A more caudal transverse section at the junction of the hindbrain and spinal cord shows the abundant VT-ir axons (small arrows) near the area postrema (AP) that cross the midline (large arrows) above the 4th ventricle (4v). (C) Sagittal section through the diencephalon shows the non-varicose fibers of the dense VT-ir preoptico-hypophyseal tract (PHT). Arrows indicate dorsal (D) and caudal (C) directions. (D) Sagittal section through the medulla near the VMN shows the hindbrain VT-ir tract with numerous varicose fibers. Arrows indicate rostral (R) and dorsal (D) directions. (E) Sagittal section through the torus semicircularis (TS) shows small scattered VT-ir fibers (arrows). (F) Sagittal section through the VMN shows varicose VT-ir axons (arrows) that surround individual motor neurons (mn). Scale bars = 50 μm (A and B); 20 μm (C and D); 10 μm (E); 15 μm (F).

F_{sex} = 25.07, p < 0.001; Tukey's tests, p = 0.02 pre spawn; p = 0.001 peak spawn; p = 0.005 post spawn) (Fig. 5B). Males also had a greater density of VT-ir fibers during peak spawn compared to all other time periods (2-way ANOVA, F_{season} = 6.63; p = 0.001; Tukey's tests, p = 0.009 pre spawn; p = 0.002 early spawn; p = 0.04 post spawn), but there was no seasonal variation in females (Tukey's tests, p > 0.05) (Fig. 5B).

The density of VT-ir fibers in the VMN was positively correlated with the number of gigantocellular somata for all fish together (Fig. 6C), as well as in males alone and females alone (Pearson Product Moment Correlation, males: r = 0.49, p = 0.01; females: r = 0.43, p = 0.02). There was no correlation between VT fiber density in the VMN and the number of magno or parvocellular somata, or somata size in any cell group (Pearson Product Moment Correlation, p > 0.05).

4. Discussion

This study demonstrates sex and seasonal variations in specific VT-ir cell groups, and in fiber densities within sensory and motor processing regions in the damselfish brain. The density of VT-ir fibers within the sensory TS and motor VMN also showed temporal variations, as well as correlations with the number of gigantocellular (TS and VMN) and parvocellular (TS) somata. VT-ir fibers within sensory and motor regions of the midbrain and hindbrain are consistent with the hypothesis that VT can influence behaviorally-relevant neuronal circuitry at multiple levels within the fish brain.

4.1. Distribution

VT-ir somata in the Hawaiian sergeant fish were found primarily within several preoptic nuclei (PPa, PPp, PMp, PMm, and PMg). This distribution is similar to those previously described in other teleosts, which largely conforms to a conserved pattern (e.g. Goodson and Bass, 2000; Miranda et al., 2003; Lema and Nevitt, 2004; Maruska et al., 2007b; Dewan et al., 2008). The Hawaiian sergeant fish also showed small VT-ir somata within the ventral tuberal region of the anterior hypothalamus, which was previously described in other fishes (e.g. Goodson and Bass, 2000; Greenwood et al., 2008). However, the prevalence, projection patterns, and function of this ventral tuberal VT-ir cell group in fishes require further study.

VT-ir fibers were found throughout the Hawaiian sergeant fish brain, but were most abundant within the area ventralis telencephali, preoptic nuclei, PHT, tegmentum, and several hindbrain nuclei (see Section 4.3). The VT-ir projection patterns in the rostral brain (telencephalon and diencephalon) are similar to that described for

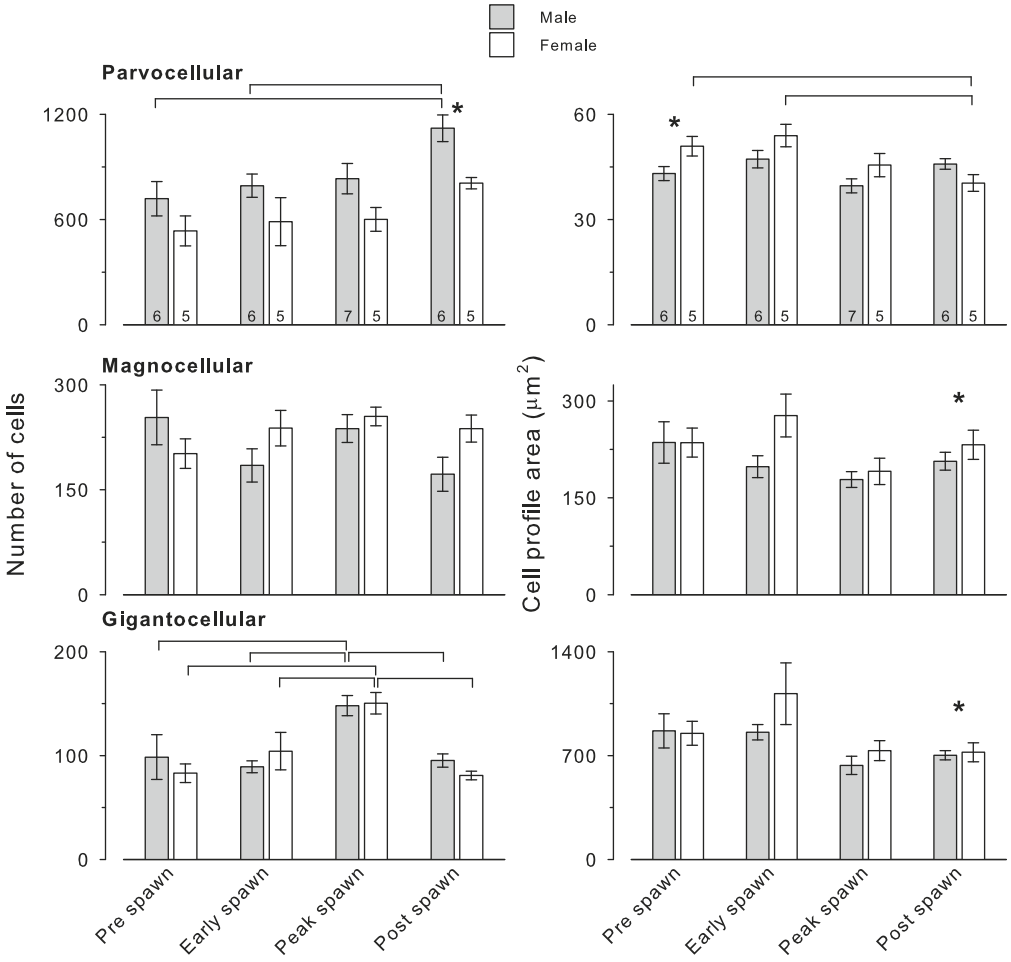

Fig. 4. Cell number and cell profile area of VT-immunoreactive (-ir) somata within the preoptic nuclei across sex and season in the Hawaiian sergeant fish, *Abudefduf abdominalis*. Sex differences were restricted to the parvocellular neurons where males had more cells during the post spawn period and females had larger cells during the pre spawn period. Seasonal variations were also found in parvocellular and gigantocellular somata groups. Most notable is the greater number of gigantocellular somata during the peak spawning season in both males and females. Bars show mean ± SE cell number and size. Numbers indicate sample size for each group. *Indicates sex differences within a period, while lines link periods that differ within a single sex (2-way ANOVA, $p < 0.05$; Tukey's test, $p < 0.05$).

other teleosts (Goodson and Bass, 2000; Miranda et al., 2003; Lema and Nevitt, 2004; Maruska et al., 2007b), but there are relatively few studies that examine fiber distributions in the fish midbrain and hindbrain for comparisons (e.g. Van den Dungen et al., 1982; Goodson and Bass, 2000; Maruska et al., 2007b; Dewan et al., 2008). VT-ir projections to the midbrain TS and hindbrain VMN were also correlated with the number of gigantocellular (TS, VMN) and parvocellular (TS) somata in the damselfish. These results are consistent with previous studies that describe extrahypothalamic projections from neurons in the nucleus preopticus magnocellularis (including gigantocellular, magnocellular, and parvocellular neurons) (Demski and Sloan, 1985; Holmqvist and Ekstrom, 1995; Saito et al., 2004; Ohya and Hayashi, 2006). However, these correlations should be interpreted with caution until the specific projection patterns of each VT-ir cell population to areas such as the midbrain TS and hindbrain VMN are demonstrated. Nevertheless, VT-ir projections to the caudal brain in the damselfish are similar to those described in the few other fishes examined, as well as in amphibians, reptiles, birds, and mammals (Kiss et al., 1987; Moore and Lowry, 1998; Goodson and Bass, 2001; Rosen et al., 2007), and may represent a conserved neuroanatomical substrate on which species- or context-specific behaviors or physiological processes can be modulated.

4.2. Sex and seasonal variations in VT-ir somata

Sex differences in VT-ir somata in the Hawaiian sergeant fish were restricted to parvocellular neurons, where males had more somata during the post spawn period, and females had larger somata during the pre spawn period. These data are consistent with other studies that show sexual dimorphisms in the parvocellular neurons of fishes (Lema and Nevitt, 2004; Ohya and Hayashi, 2006; Maruska et al., 2007b) as well as regions homologous to the PPa, PPp, and PMp of teleost fishes (see Goodson and Bass, 2001). Sex differences in the VT and VP neurosecretory system are well established in a wide variety of vertebrates, and are most often related to gonadal sex hormones (see Goodson and Bass, 2001).

The Hawaiian sergeant fish also showed seasonal variations in the number (males) and size (females) of parvocellular VT-ir somata. In addition to social behavior, VT in fishes is known to function in osmoregulation, cardiovascular response, stress response and metabolism (Balment et al., 2006), and thus the seasonal variations in number and size of parvocellular neurons in the Hawaiian sergeant fish could be related to any of these social, environmental, or physiological factors. Previous studies demonstrate that parvocellular VT neurons show variations in number, size, or gene expression in response to both environmental and physiological cues. For example, variations in salinity cause changes in parvo cell

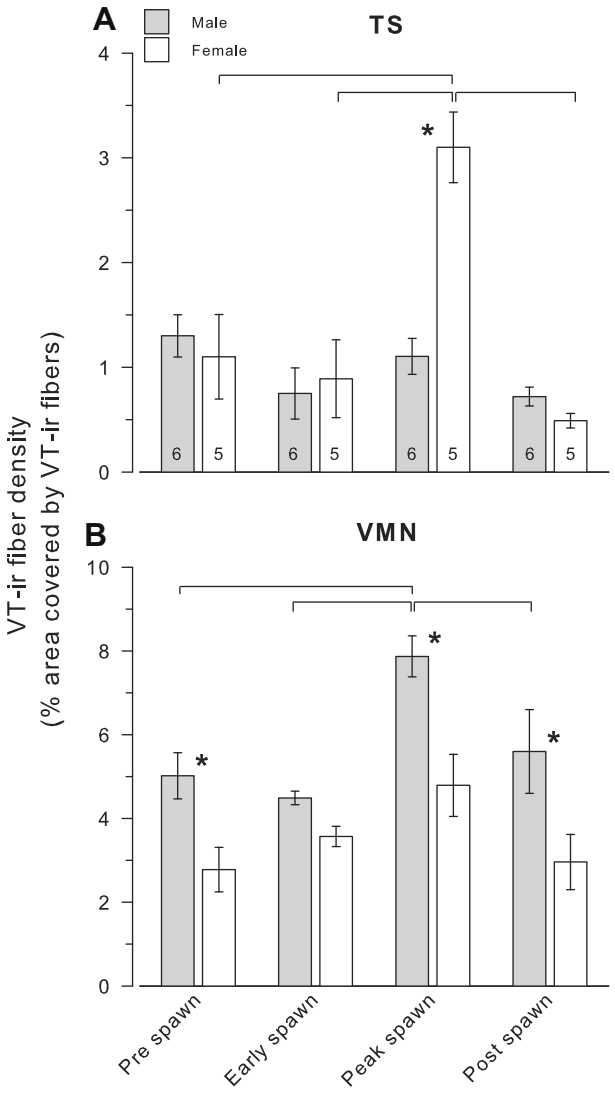

Fig. 5. VT-immunoreactive (-ir) fiber densities within the sensory torus semicircularis of the midbrain (A) and the vagal motor nucleus of the hindbrain (B) across sex and season in the Hawaiian sergeant fish, *Abudefduf abdominalis*. Females had greater fiber innervation to the torus semicircularis (TS) during the peak spawning season compared to males, while males had greater fiber densities in the vagal motor nucleus (VMN) compared to females. Seasonally, fiber densities in the TS of females were higher during peak spawning, and fiber densities in the VMN of males were higher during peak spawning compared to all other times. Fiber densities are expressed as the percent area covered by VT-ir axons per 360 μm^2 area. Bars show mean ± SE and numbers indicate sample size for each group. *Indicates sex differences within a period, while lines link periods that differ within a single sex (2-way ANOVA, $p < 0.05$; Tukey's test, $p < 0.05$).

numbers in pupfish (*Cyprinodon nevadensis*) (Lema, 2006), stress was shown to increase VT gene expression in parvo, but not magnocellular neurons in the rainbow trout (*Oncorhynchus mykiss*) (Gilchriest et al., 2000), and parvocellular VT neurons are involved in the regulation of cortisol release via the actions of VT on the hypothalamic–pituitary–interrenal axis (Olivereau and Olivereau, 1990; Gilchriest et al., 2000; Balment et al., 2006). Males and females of the same species often respond differently to stressors (Overli et al., 2006), and it is possible that one sex is more affected than the other to some environmental change due to different physiological demands at different times of the year, which may help explain the temporal patterns seen in the Hawaiian sergeant fish parvocellular neurons. Glucocorticoids (i.e. corticosterone and cortisol) are also known to influence VT-mediated neuronal activity (Rose et al., 1995; Rose and Moore, 2002), and therefore provide a possi-

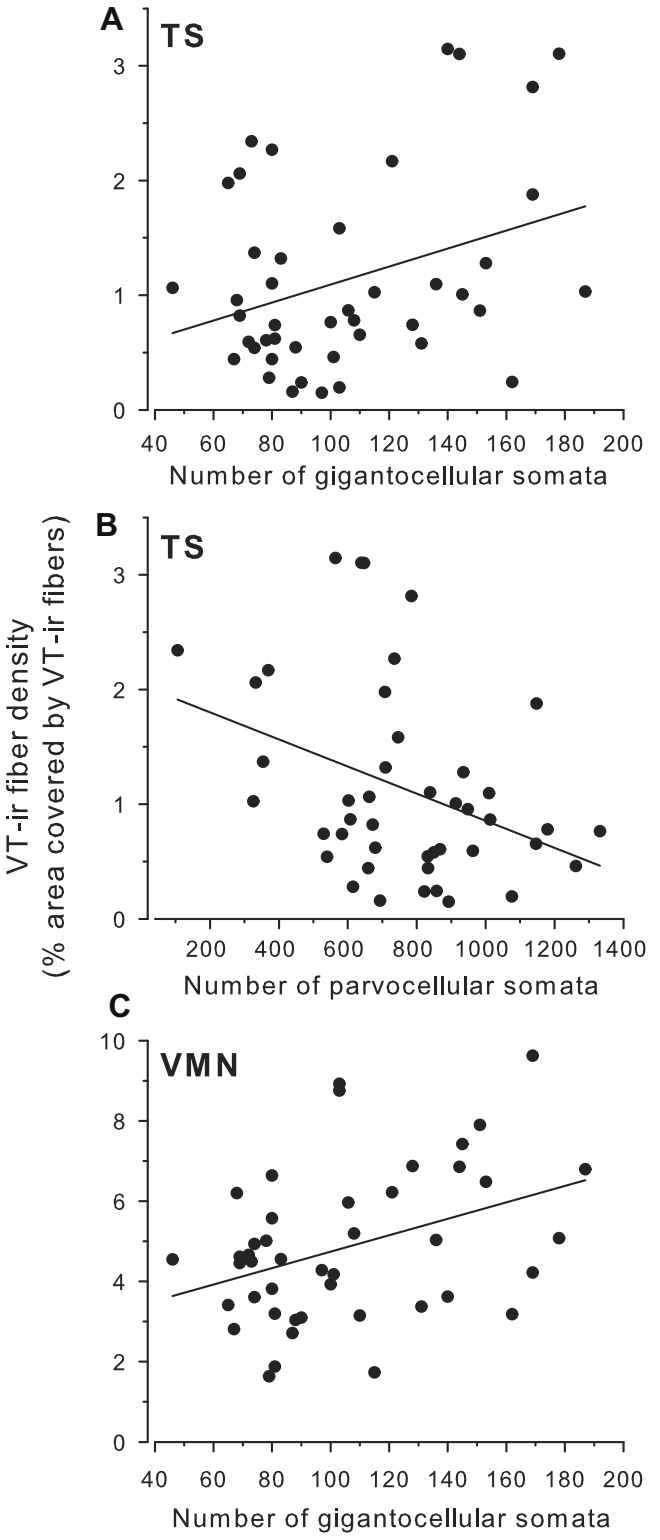

Fig. 6. Correlation between VT-immunoreactive (-ir) somata and fiber densities within the torus semicircularis of the midbrain and vagal motor nucleus of the hindbrain in the Hawaiian sergeant fish, *Abudefduf abdominalis*. (A) VT-ir fiber density in the torus semicircularis (TS) was positively correlated with the number of gigantocellular somata (Pearson Product Moment Correlation, $r = 0.34$, $p = 0.02$). (B) VT-ir fiber density in the TS was also negatively correlated with the number of parvocellular somata (Pearson Product Moment Correlation, $r = -0.35$, $p = 0.02$). (C) VT-ir fiber density in the vagal motor nucleus was positively correlated with the number of gigantocellular somata (Pearson Product Moment Correlation, $r = 0.38$, $p = 0.01$). Fiber densities are expressed as the percent area covered by VT-ir axons per 360 μm^2 area. Each point represents a single fish ($n = 44$) and linear regression lines are shown on each plot.

ble mechanism for modulation of behaviors by the presence of stressors that warrants further investigation across taxa.

The most notable seasonal variation in the Hawaiian sergeant fish VT system was the greater number of gigantocellular neurons during the peak spawning period in both males and females. The gigantocellular VT cell group is thus far found only in teleost fishes, but the function of these neurons is not yet known. However, several studies do show correlations between gigantocellular neurons and reproduction. For example, gigantocellular somata numbers were elevated during the peak spawning season in the halfspotted goby (*Asterropteryx semipunctata*) (Maruska et al., 2007b), seasonal changes in VT expression were most predominant in gigantocellular neurons in masu salmon (*Oncorhynchus masou*) (Ota et al., 1999), castration affected only gigantocellular soma size in bluehead wrasse (*Thalassoma bifasciatum*) (Semsar and Godwin, 2003), and increased VT mRNA expression in the gigantocellular region was positively correlated with agonistic and reproductive behaviors in the African cichlid fish (*Astatotilapia burtoni*) (Greenwood et al., 2008). Thus the greater number of VT gigantocellular somata during peak spawning in the damselfish may also be related to some aspect of their reproductive physiology, behavior, or social environment. Further physiological and behavioral studies are needed to directly test the hypothesis that parvo, magno, and gigantocellular VT groups serve different functions in fishes.

4.3. VT-immunoreactivity in motor and sensory regions

VT-ir axons innervate several sensory and motor processing regions in the Hawaiian sergeant fish brain, which is consistent with the hypothesis that both sensory and motor processing can be influenced by VT at multiple levels in the fish brain (Rose and Moore, 2002; Moore and Rose, 2002). The presence of VT within these regions alone does not provide definitive evidence of physiological action or behavioral function because neuropeptides released in one region can act by diffusion or volume transmission in areas located many microns away (Landgraf and Neumann, 2004). However, many of the same sensory and motor regions of the brain that contain VT-ir axons in this study are also known to express V1a receptors or VT binding sites in several taxa (Moons et al., 1989; Ostrowski et al., 1994; Boyd, 1997; Lewis et al., 2005).

Neuroanatomical, physiological and behavioral studies demonstrate that VT and VP play a role in both vocal behavior and auditory processing across taxa (Dubois-Dauphin et al., 1987; Penna et al., 1992; Boyd, 1994; Goodson and Bass, 2000). VT-ir axons in the Hawaiian sergeant fish were also localized to the auditory-mechanosensory TS of the midbrain. Hawaiian sergeant fish produce low frequency sounds during agonistic interactions and courtship (Maruska et al., 2007a), and vocal-acoustic communication is important for many damselfishes. The mechanism of sound production remains unknown in most damselfishes, but is hypothesized to involve movements of the pharyngeal jaw apparatus and amplification by the swim bladder (Rice and Lobel, 2003). A recent study in another damselfish species showed that sound production involves a sonic ligament and movements of the jaw that may be an exaptation of the feeding mechanism (Parmentier et al., 2007). VMN neurons in fishes innervate the pharyngeal jaw muscles, and therefore VT-ir axons in this region of the Hawaiian sergeant brain could possibly influence vocal output. The mammalian homolog VP is also known to have powerful excitatory actions on hindbrain motor neurons involved in feeding and other visceral functions in mammals (Mo et al., 1992; Reymond-Marron et al., 2006), and thus VT may have conserved distributions in these hindbrain regions. Alternatively, VT in the VMN could be involved in the control of autonomic responses related to circulation, digestion, or respiration that may undergo seasonal changes in physiological demands (e.g. viscerosensory function), or be part of a primitive social circuit that regulates social and emotional behaviors (Thompson et al., 2008).

4.4. Sex and seasonal variations in VT-ir fiber densities

The Hawaiian sergeant fish showed distinct seasonal variations in VT innervation to the sensory TS. While changes in VT somata (size, number, or gene expression) according to season, sex, reproductive or social status exist in many vertebrates, this study is the first to quantify sex and seasonal variations in VT innervation to caudal brain regions in a teleost fish. VT-ir axons and VT receptors are found within midbrain auditory regions of mammals, amphibians, and fish (Dubois-Dauphin et al., 1987; Moons et al., 1989; Goodson and Bass, 2000; Boyd, 1997), and VT is known to influence auditory processing in the midbrain of amphibians (Penna et al., 1992). Thus increased VT innervation within the TS of female Hawaiian sergeant fish during the peak reproductive period may influence detection of acoustic and hydrodynamic cues from males during courtship and spawning behaviors similar to that described in the tectum of the roughskin newt (*Taricha granulosa*) where VT may prime the visual system during the breeding season (Zoeller and Moore, 1986). VT-immunoreactivity is also steroid-sensitive across taxa (Boyd, 1997; Panzica et al., 2001; Goodson and Bass, 2001) and seasonal changes in VT-ir somata and fiber innervation to auditory sensory regions may be regulated by circulating gonadal steroids or locally synthesized neurosteroids that vary across the reproductive cycle (Do-Rego et al., 2006).

Male Hawaiian sergeant fish showed greater VT innervation to the hindbrain VMN compared to females, as well as greater fiber densities during the peak spawning period. Male damselfish are generally more vocal than females as they produce several different types of agonistic and reproductive sounds (Myrberg and Ladich, 2006), which may explain the greater VMN VT-ir innervation in male Hawaiian sergeant fish compared to females. Alternatively, VT in the VMN of the Hawaiian sergeant fish may not be related to vocal behavior at all, but rather associated with hindbrain autonomic processes that influence a primitive social circuit possibly controlling social and emotional behaviors across vertebrates (Thompson et al., 2008).

In summary, the present study shows sex and seasonal variations in several VT cell groups and fiber projections in the Hawaiian sergeant fish that are correlated with temporal reproduction. VT-ir fibers were also found within sensory and motor regions of the midbrain and hindbrain, which provides neuroanatomical support for the hypothesis that VT can influence processing at multiple levels within the fish brain. Future studies that localize VT receptors and test the physiological and behavioral effects of VT neuronal variations in single fish species are needed to determine the biological function and evolution of this important nonapeptide.

Acknowledgments

I thank Matthew Grober for the generous gift of VT antiserum, Tim Tricas for his support and discussions during this project, K.A. Peyton for help with fish collections, A.K. Dewan and two anonymous reviewers for insightful comments that helped to improve the manuscript, and the A.L. Tester Foundation and an Achievement Rewards for College Scientists (ARCS) award for partial funding support.

References

Balment, R.J., Lu, W., Weybourne, E., Warne, J.M., 2006. Arginine vasotocin a key hormone in fish physiology and behavior: a review with insights from mammalian models. Gen. Comp. Endocrinol. 147, 9–16.

Boyd, S.K., 1994. Arginine vasotocin facilitation of advertisement calling and call phonotaxis in bullfrogs. Horm. Behav. 28, 232–240.
Boyd, S.K., 1997. Brain vasotocin pathways and the control of sexual behaviors in the bullfrog. Brain Res. Bull. 44, 345–350.
Braford Jr., M.R., Northcutt, R.G., 1983. Organization of the diencephalon and pretectum of the ray finned fishes. In: Davis, R.E., Northcutt, R.G. (Eds.), Fish Neurobiology. University of Michigan, Ann Arbor, MI, pp. 117–164.
Demski, L.S., Sloan, H.E., 1985. A direct magnocellular-preopticospinal pathway in goldfish: implications for control of sex behavior. Neurosci. Lett. 55, 283–288.
Dewan, A.K., Maruska, K.P., Tricas, T.C., 2008. Arginine vasotocin neuronal populations among congeneric territorial and shoaling reef butterflyfishes: species, sex and reproductive season comparisons. J. Neuroendocrinol. 20, 1382–1394.
Do-Rego, J.L., Acharjee, S., Seong, J.Y., Galas, L., Alexandre, D., Bizet, P., Burlet, A., Kwon, H.B., Luu-The, V., Pelletier, G., Vaudry, H., 2006. Vasotocin and mesotocin stimulate the biosynthesis of neurosteroids in the frog brain. J. Neurosci. 26, 6749–6760.
Dubois-Dauphin, M., Tribollet, E., Dreifuss, J.J., 1987. A sexually dimorphic vasopressin innervation of auditory pathways in the guinea pig brain. Brain Res. 437, 151–156.
Foran, C.M., Bass, A.H., 1998. Preoptic AVT immunoreactive neurons of a teleost fish with alternative reproductive tactics. Gen. Comp. Endocrinol. 111, 271–282.
Foran, C.M., Bass, A.H., 1999. Preoptic GnRH and AVT: axes for sexual plasticity in teleost fish. Gen. Comp. Endocrinol. 116, 141–152.
Gilchriest, B.J., Tipping, D.R., Hake, L., Levy, A., Baker, B.I., 2000. The effects of acute and chronic stresses on vasotocin gene transcripts in the brain of rainbow trout (*Oncorhynchus mykiss*). J. Neuroendocrinol. 12, 795–801.
Godwin, J., Sawby, R., Warner, R.R., Crews, D., Grober, M.S., 2000. Hypothalamic arginine vasotocin mRNA abundance variation across sexes and with sex change in a coral reef fish. Brain Behav. Evol. 55, 77–84.
Goodson, J.L., Bass, A.H., 2001. Social behavior functions and related anatomical characteristics of vasotocin/vasopressin systems in vertebrates. Brain Res. Rev. 35, 246–265.
Goodson, J.L., Bass, A.H., 2000. Vasotocin innervation and modulation of vocal-acoustic circuitry in the teleost *Porichthys notatus*. J. Comp. Neurol. 422, 363–379.
Greenwood, A.K., Wark, A.R., Fernald, R.D., Hofmann, H.A., 2008. Expression of arginine vasotocin in distinct preoptic regions is associated with dominant and subordinate behavior in an African cichlid fish. Proc. Biol. Sci. 275, 2393–2402.
Grober, M.S., George, A.A., Watkins, K.K., Carneiro, L.A., Oliveira, R.F., 2002. Forebrain AVT and courtship in a fish with male alternative reproductive tactics. Brain Res. Bull. 57, 423–425.
Helfrich, P., 1958. The early life history and reproductive behavior of the maomao, *Abudefduf abdominalis* (Quoy and Gaimard). Ph.D. Dissertation, Zoology Dept., University of Hawai'i at Manoa, 228 pp.
Holmqvist, B.I., Ekstrom, P., 1995. Hypophysiotrophic systems in the brain of the Atlantic salmon. Neuronal innervations of the pituitary and the origin of pituitary dopamine and nonapeptides identified by means of combined carbocyanine tract tracing and immunocytochemistry. J. Chem. Neuroanat. 8, 125–145.
Kiss, J.Z., Voorhuis, T.A.M., van Eekelen, J.A.M., de Kloet, E.R., de Wied, D., 1987. Organization of vasotocin-immunoreactive cells and fibers in the canary brain. J. Comp. Neurol. 263, 347–364.
Landgraf, R., Neumann, I.D., 2004. Vasopressin and oxytocin release within the brain: a dynamic concept of multiple and variable modes of neuropeptide communication. Front. Neuroendocrinol. 25, 150–176.
Lema, S.C., 2006. Population divergence in plasticity of the AVT system and its association with aggressive behaviors in a Death Valley pupfish. Horm. Behav. 50, 183–193.
Lema, S.C., Nevitt, G.A., 2004. Variation in vasotocin immunoreactivity in the brain of recently isolated populations of a Death Valley pupfish, *Cyprinodon nevadensis*. Gen. Comp. Endocrinol. 135, 300–309.
Lewis, C.M., Dolence, E.K., Hubbard, C.S., Rose, J.D., 2005. Identification of roughskin newt medullary vasotocin target neurons with a fluorescent vasotocin conjugate. J. Comp. Neurol. 491, 381–389.
Lim, M.M., Young, L.J., 2006. Neuropeptidergic regulation of affiliative behavior and social bonding in animals. Horm. Behav. 50, 506–517.
Maruska, K.P., 2007. Acoustic communication, auditory processing, and neuropeptide modulation of sensory systems in coral reef fishes. Ph.D. Dissertation, University of Hawai'i at Manoa, Honolulu, HI, 302 pp.
Maruska, K.P., Tricas, T.C., 2007. Gonadotropin-releasing hormone (GnRH) and receptor distributions in the visual processing regions of four coral reef fishes. Brain Behav. Evol. 70, 40–56.
Maruska, K.P., Boyle, K.S., Dewan, L.R., Tricas, T.C., 2007a. Sound production and spectral hearing sensitivity in the Hawaiian sergeant damselfish, *Abudefduf abdominalis*. J. Exp. Biol. 210, 3990–4004.
Maruska, K.P., Mizobe, M.H., Tricas, T.C., 2007b. Sex and seasonal co-variation of arginine vasotocin (AVT) and gonadotropin-releasing hormone (GnRH) neurons in the brain of the halfspotted goby. Comp. Biochem. Physiol. A 147, 129–144.
Miranda, J.A., Oliveira, R.F., Carneiro, L.A., Santos, R.S., Grober, M.S., 2003. Neurochemical correlates of male polymorphism and alternative reproductive tactics in the Azorean rock-pool blenny, *Parablennius parvicornis*. Gen. Comp. Endocrinol. 132, 183–189.
Mo, Z.L., Katafuchi, T., Muratani, H., Hori, T., 1992. Effects of vasopressin and angiotensin II on neurons in the rat dorsal motor nucleus of the vagus, *in vitro*. J. Physiol. 458, 561–577.
Moons, L., Cambre, M., Batten, T.F.C., Vandesande, F., 1989. Autoradiographic localization of binding sites for vasotocin in the brain and pituitary of the sea bass, *Dicentrarchus labrax*. Gen. Comp. Endocrinol. 73, 270–283.
Moore, F.L., Lowry, C.A., 1998. Comparative neuroanatomy of vasotocin and vasopressin in amphibians and other vertebrates. Comp. Biochem. Physiol. C Pharmacol. Toxicol. Endocrinol. 119, 251–260.
Moore, F.L., Rose, J.D., 2002. Sensorimotor processing model: how vasotocin and corticosterone interact and control reproductive behavior in an amphibian. In: Pfaff, D., Arnold, A., Etgen, A., Fahrbach, S., Rubin, R. (Eds.), Hormones, Brain and Behavior, vol. II. Elsevier Science, pp. 515–544.
Myrberg Jr., A.A., Ladich, F., 2006. Reproductive behavior and acoustical interactions. In: Ladich, F., Collin, S.P., Moller, P., Kapoor, B.G. (Eds.), Communication in Fishes. Science Publishers, Enfield, NH, pp. 149–176.
Ohya, T., Hayashi, S., 2006. Vasotocin/isotocin-immunoreactive neurons in the medaka fish brain are sexually dimorphic and their numbers decrease after spawning in the female. Zool. Sci. 23, 23–29.
Oliveira, R.F., Ros, A.F.H., Goncalves, D.M., 2005. Intra-sexual variation in male reproduction in teleost fish: a comparative approach. Horm. Behav. 48, 430–439.
Olivereau, M., Olivereau, J., 1990. Effect of pharmacological adrenalectomy on corticotropin-releasing factor-like and arginine vasotocin immunoreactivities in the brain and pituitary of the eel: immunocytochemical study. Gen. Comp. Endocrinol. 80, 199–215.
Ostrowski, N.L., Lolait, S.J., Young, W.S., 1994. Cellular localization of vasopressin V1a receptor messenger ribonucleic acid in adult male rat brain, pineal, and brain vasculature. Endocrinology 135, 1511–1528.
Ota, Y., Ando, H., Ueda, H., Urano, A., 1999. Differences in seasonal expression of neurohypophysial hormone genes in ordinary and precocious male masu salmon. Gen. Comp. Endocrinol. 116, 40–48.
Overli, O., Sorensen, C., Nilsson, G.E., 2006. Behavioral indicators of stress-coping style in rainbow trout: do males and females react differently to novelty? Physiol. Behav. 87, 506–512.
Panzica, G.C., Aste, N., Castagna, C., Viglietti-Panzica, C., Balthazart, J., 2001. Steroid-induced plasticity in the sexually dimorphic vasotocinergic innervation of the avian brain: behavioral implications. Brain Res. Rev. 37, 178–200.
Parhar, I.S., Tosaki, H., Sakuma, Y., Kobayashi, M., 2001. Sex differences in the brain of goldfish: gonadotropin-releasing hormone and vasotocinergic neurons. Neuroscience 104, 1099–1110.
Parmentier, E., Colleye, O., Fine, M.L., Frederich, B., Vandewalle, P., Herrel, A., 2007. Sound production in the clownfish *Amphiprion clarkii*. Science 316, 1006.
Penna, M., Capranica, R.R., Somers, J., 1992. Hormone-induced vocal behavior and midbrain auditory sensitivity in the green treefrog *Hyla cinerea*. J. Comp. Physiol. A 170, 73–82.
Reymond-Marron, I., Tribollet, E., Raggenbass, M., 2006. The vasopressin-induced excitation of hypoglossal and facial motoneurons in young rats is mediated by V1a but not V1b receptors, and is independent of intracellular calcium signaling. Eur. J. Neurosci. 24, 1565–1574.
Rice, A.N., Lobel, P.S., 2003. The pharyngeal jaw apparatus of the Cichlidae and Pomacentridae: function in feeding and sound production. Rev. Fish Biol. 13, 433–444.
Rose, J.D., Moore, F.L., 2002. Behavioral neuroendocrinology of vasotocin and vasopressin and the sensorimotor processing hypothesis. Front. Neuroendocrinol. 23, 317–341.
Rose, J.D., Kinnaird, J.R., Moore, F.L., 1995. Neurophysiological effects of vasotocin and corticosterone on medullary neurons: implications for hormonal control of amphibian courtship behavior. Neuroendocrinology 62, 406–417.
Rosen, G.J., De Vries, G.J., Goldman, S.L., Goldman, B.D., Forger, N.G., 2007. Distribution of vasopressin in the brain of the eusocial naked mole-rat. J. Comp. Neurol. 500, 1093–1105.
Saito, D., Komatsuda, M., Urano, A., 2004. Functional organization of preoptic vasotocin and isotocin neurons in the brain of rainbow trout: central and neurohypophysial projections of single neurons. Neuroscience 124, 973–984.
Semsar, K., Godwin, J., 2003. Social influences on the arginine vasotocin system are independent of gonads in a sex-changing fish. J. Neurosci. 23, 4386–4393.
Thompson, R.R., Walton, J.C., Bhalla, R., George, K.C., Beth, E.H., 2008. A primitive social circuit: vasotocin-substance P interactions modulate social behavior through a peripheral feedback mechanism in goldfish. Eur. J. Neurosci. 27, 2285–2293.
Van den Dungen, H.M., Buijs, R.M., Pool, C.W., Terlou, M., 1982. The distribution of vasotocin and isotocin in the brain of the rainbow trout. J. Comp. Neurol. 212, 146–157.
Zoeller, R.T., Moore, F.L., 1986. Correlation between immunoreactive vasotocin in optic tectum and seasonal changes in reproductive behavior of male rough-skinned newts *Taricha granulosa*. Horm. Behav. 20, 148–154.